Optical and electron-energy-loss studies of the monomeric and dimeric phases of decamethylferrocenium tetracyanoquinodimethanide, (DMeFc)(TCNQ)

D. B. Tanner
Department of Physics, Ohio State University, Columbus, Ohio 43210

Joel S. Miller,* M. J. Rice, and J. J. Ritsko
Xerox Webster Research Center, Rochester, New York 14644

(Received 10 October 1979)

The optical properties of the two crystallographic phases of 1:1 decamethylferrocenium tetracyanoquinodimethanide, (DMeFc)(TCNQ), have been measured from 0.1 to 10 eV. One phase consists of isolated paramagnetic TCNQ anion monomers while the other contains isolated diamagnetic dimers. The spectrum of the monomeric phase exhibits a strong localized monomer exciton which is not normally observed in solid TCNQ salts, while the dimeric phase shows a charge-transfer excitation as well as a shifted local exciton. From the frequency-dependent conductivity of the dimeric phase the effective on-site Coulomb interaction and the transfer matrix element are measured to be 1.0 and 0.27 eV, respectively. The infrared absorption spectrum of the dimeric phase shows an unusual activity of the symmetric phonon modes due to the interaction of these modes with the radical electron, whereas in the monomeric phase only normally infrared active phonons are observed. In electron-energy-loss measurements an anomalous momentum dependence of the line shape of the monomeric exciton was observed. This result is attributed to a dielectric effect caused by the decrease in strength of local excitons with increasing momentum.

I. INTRODUCTION

The organic radical-ion salt decamethylferrocenium tetracyanoquinodimethanide, (DMeFc)(TCNQ) {DMeFc = $Fe[C_5(CH_3)_5]_2$} has the unusual property of crystallizing in two quite different structural forms.[1,2] In one of these forms,[1] individual $TCNQ^-$ monomers are placed between $DMeFc^+$ ions. Other $DMeFc^+$ ions are adjacent to the $TCNQ^-$ monomer along the long axis of this ion. In the second phase,[2] pairs or dimers of $TCNQ^-$ ions are placed between $DMeFc^+$ ions. This basic structural unit, $(DMeFc)^+$ $(TCNQ)^-$ $(TCNQ)^-(DMeFc)^+$ is arranged in a herringbone fashion in the solid. The structures of these two phases are shown in Fig. 1. Because of this structural variety, (DMeFc)(TCNQ) is an important model system for the investigation of the electronic structure of the TCNQ molecule in the solid state. In the monomeric phase[1] the vibrational modes and the low-lying electronic excitations of an individual $TCNQ^-$ molecule can be observed. In the dimeric phase[2] the interactions between adjacent $TCNQ^-$

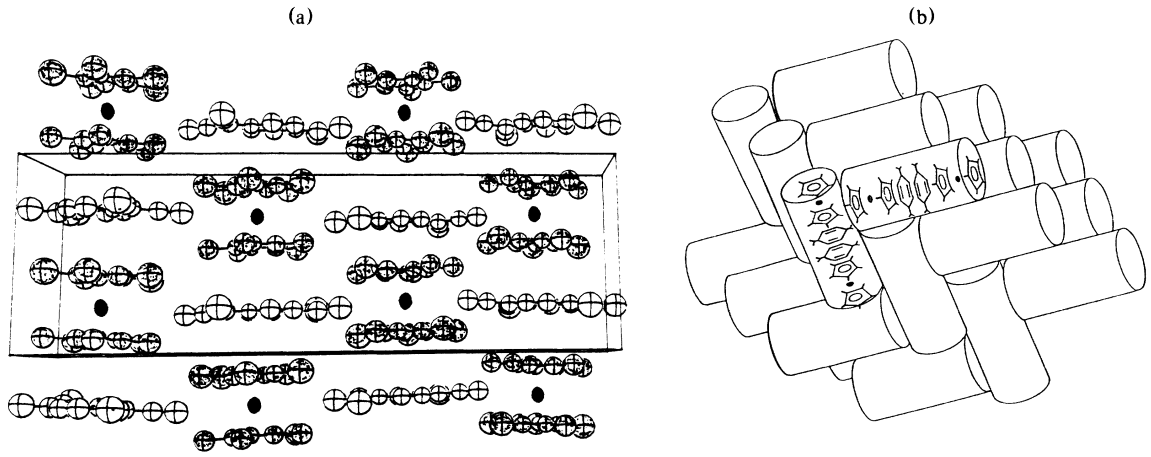

FIG. 1. (a) Structure of the monomeric phase (DMeFc) (TCNQ). View is down the $\vec{c}$ axis. The stacks are along the $\vec{a}$ axis. From Ref. 1. (b) Schematic view of the dimeric phase $(DMeFc^+)_2(TCNQ)_2^2$. Each "log" contains one dimeric unit. From Ref. 2.

ions may be studied. These interactions include the overlap of the electronic wave functions on adjacent molecular sites, the "on-site" Coulomb interaction between electrons occupying the same TCNQ molecular orbital and the interaction of the radical electron with the vibrational modes of the molecule (i.e., the electron-phonon interaction). This paper describes the optical properties of these two phases. The monomeric phase was studied in thin-film form by optical transmission and electron-energy-loss techniques while the dimeric phase was investigated by polarized reflectance studies of single crystals.

The next section of this paper describes materials preparation, materials characterization, and optical techniques. The data are presented in the third section while detailed discussion is given in the fourth section. The results and conclusions are summarized in the final section.

II. EXPERIMENTAL TECHNIQUE

A. Materials synthesis

The preparation of the 1:1 $\{Fe[C_5(CH_3)_5]_2\}$ TCNQ complexes has previously been described.[1,2] The dimeric phase occurs when crystals are grown by slow evaporation from acetonitrile solution. These crystals are relatively large (ca. $0.2 \times 0.1 \times 0.02$ cm^3) and are the chemically more stable of the two phases. Quick growth or vapor deposition results in the formation of the monomeric phase. This phase is susceptible to oxygen attack, with an accompanying change of color from yellow-green to red.[2]

The monomeric phase was studied in evaporated thin-film form. These films were deposited on glass, quartz, NaCl, and Parafilm substrates, via resistive heating of a tantalum boat. During evaporation the pressure rose from 5×10^{-6} to 1×10^{-4} Torr. These films were between 1500 and 6000 Å thick, as monitored by a calibrated quartz-crystal thickness monitor. Free-standing films needed for the transmission electron-energy-loss studies were prepared by floating off films deposited on microscope slides onto the surface of water from which they were removed and supported by a standard 3-mm-diameter gold electron microscope grid.

B. Materials characterization

1. Structure

The structures of the two phases have been recently reported.[1,2] The crystal growth habit of the dimeric phase is such that flat plates are obtained, with the largest face containing the a and b axes of the monoclinic unit cell. The polarized reflectance measurements were made on this face. The studies of the monomeric phase were carried out on freshly sublimed thin films. To confirm that the polycrystalline thin films were isomorphous to the bulk structure, an electron diffraction pattern was obtained and compared to the powder x-ray-diffraction pattern. The electron diffraction measurements were made in the electron-energy-loss spectrometer as well as with a commercial electron microscope. This comparison indicated that the thin films are isomorphous to the monomeric phase.

Upon standing in air the yellow-green film turns red. Electron diffraction measurements on the red film gave a pattern identical to those from the yellow-green film. Thus, upon transformation from the yellow-green to red phase the unit cell does not appear to be significantly altered.[2]

2. Magnetic properties

The two phases have quite different magnetic properties. The dimeric complex behaves magnetically as a simple $S = \frac{1}{2}$ system (per iron) with no antiferromagnetic coupling observed in single crystals for the studied temperature range, 1.5– 300 K.[2] In contrast the monomeric phase behaves as a metamagnet below 2.55 K.[3] In applied fields below 1500 Oe, this complex is an antiferromagnet whereas above 1500 Oe it is ferromagnetic.

C. Optical techniques

Different optical techniques were employed to study the two 1:1 (DMeFc)(TCNQ) phases. The evaporated films of the monomeric phase were investigated by optical transmission and electron energy-loss measurements. A Perkin-Elmer 283 infrared spectrophotometer was employed over 0.025– 0.5 eV (200– 4000 cm^{-1}) while a Cary 17 spectrophotometer covered the 0.5– 6.2 eV (4000–50 000 cm^{-1}) region. A custom built high-resolution spectrometer enabled the energy-loss spectra of 80-keV electrons transmitted through the films to be measured between 0.6 and 11.0 eV with a resolution of 0.1 eV as a function of momentum transfer from 0.1 to 0.7 Å^{-1}.

The dimeric phase was studied using polarized reflectance on single crystals. These measurements were made with a Perkin-Elmer model 16U grating monochromator. Four gratings were used to cover photon energies from 0.09 eV (700 cm^{-1}) to 4.7 eV (37 000 cm^{-1}) with a resolution of $\Delta\omega/\omega \sim 10^{-3}$. Long pass and bandpass filters eliminated unwanted orders of diffraction. The exit slit of the monochromator was imaged onto the crystal with a large spherical mirror and a second such mirror focused the reflected light onto the detector. The detector was a thermocouple below 0.5 eV (4000 cm^{-1}), a PbS

photoconductor between 0.5 and 1.9 eV (4000–15 000 cm^{-1}), and a photomultiplier above 1.9 eV (15 000 cm^{-1}). A wire grid polarizer was used in the middle infrared, and dichroic polarizers were used in the near-infrared through ultraviolet regions.

III. EXPERIMENTAL RESULTS

In this section of the paper we present the optical data obtained on the two phases of (DMeFc)(TCNQ), deferring extended discussion of these data until the following section. We first describe the results for the monomeric phase: solution spectra, thin-film optical transmission, and thin-film electron-energy-loss measurements. Then we present the results for the dimeric phase, obtained by polarized reflectance measurements.

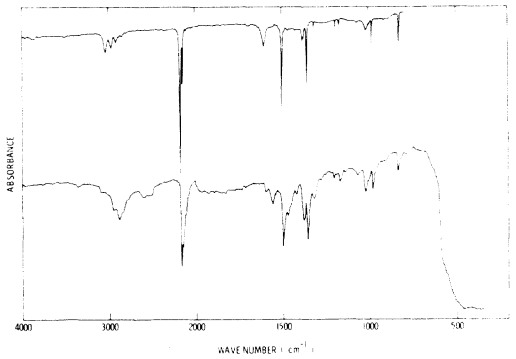

FIG. 2. Absorbance (increasing downwards) vs frequency (increasing to the left) for (DMeFc)(TCNQ) in dichloromethane solution (upper trace) and for the monomeric phase in thin-film form (lower trace).

A. Solution spectra

Solutions of either phase (at $\sim 10^{-4}M$) have transmission spectra which can be decomposed into the spectra of isolated $DMeFc^+$ and monomeric $TCNQ^-$ ions.[4–6] In the infrared region, these samples exhibit the clean spectra shown as the upper trace in Fig. 2. The observed frequencies are given in the first column of Table I. No absorption is observed between 0.5 and 1.2 eV. Between 1.38 eV (11 100 cm^{-1}) and 2.25 eV (18 200 cm^{-1}) the spectrum is dominated by the well-known[4,5] intense absorption with a maximum at 1.45 eV (11 660 cm^{-1}) characteristic of the $A_{1g} \rightarrow B_{1u}$ molecular orbital transition[7] with a strong vibronic progression. This re-

TABLE I. Observed molecular vibration frequencies in (DMeFc)(TCNQ) (cm^{-1}).

Dichloromethane solution	Monomeric phase (film)	Dimeric phase $\vec{E} \parallel \vec{a}$	Dimeric phase $\vec{E} \parallel \vec{b}$
3050	2960		
2925	2890		
2850	2840		
	2179		
2181			2171
	2160	2171	
2155	2152		2146
1609	1598	1591	
1506	1500	1511	
1475	1470		
	1380		
		1360	1362
1362	1359		
		1175	1175
1020	1020		
	1002		
988	980		
830	833	825	

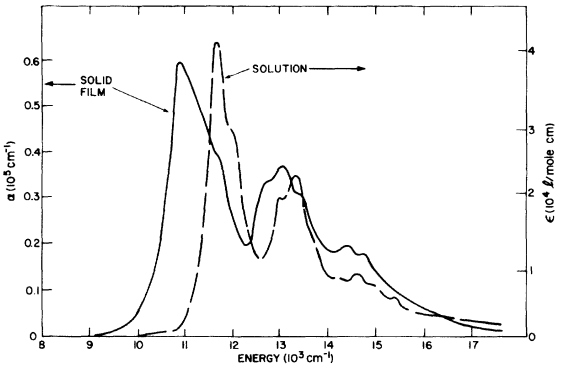

FIG. 3. The absorption coefficient α of a thin film of the monomeric phase and the molar extinction coefficient ϵ of an acetonitrile solution of (DMeFc)(TCNQ) vs frequency.

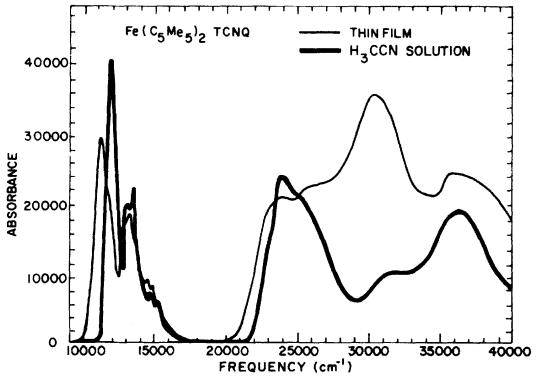

FIG. 4. The absorbance of a solution and of a film of the monomeric phase of (DMeFc)(TCNQ) between 10000 cm^{-1} (1.2 eV) and 40000 cm^{-1} (5 eV).

gion is shown in Fig. 3 while the entire near-infrared–near-ultraviolet region is shown in Fig. 4. The frequencies of the absorption maxima are given in the first column of Table II. Aggregation of the ions is not observed in these solvents. The absorptions above 2.25 eV can be reduced to the sum of $DMeFc^+$ and $TCNQ^-$ absorptions.[4,6,14,16] The $Fe(II)[C_5(CH_3)_5]_2$ complex shows solution absorption at 37600 and 44800 cm^{-1} while the $Fe(III)[C_5(CH_3)_5]_2$ complex has absorption at 31800, 36200, 41000, and 45800 cm^{-1}. A discussion of the electronic properties of these species is given by Duggan and Hendrickson.[6]

B. Thin-film spectra of the monomeric phase

Infrared spectra of freshly prepared thin films of the monomeric phase on NaCl substrates were very similar to the solution data. The major difference, as shown in the lower trace in Fig. 2, were shifting to lower frequencies and broadening of the absorption lines. The frequencies are tabulated in the second column of Table I.

Extension of the infrared data to lower frequency was provided by using a Parafilm substrate, which transmits above 200 cm^{-1}; however, no significant structure was observed in this region.

The thin-film absorption spectrum between 1.24–5.0 eV (10000–40000 cm^{-1}) is illustrated in Figs. 3 and 4. No absorption is observed between 0.5–1.24 eV (4000–10000 cm^{-1}). Between 1.24–2.23 eV (10000–18000 cm^{-1}) the characteristic $TCNQ^-$ vibronically coupled multiplet appears relatively intact except for a broadening of the lowest-energy absorption and a shift to lower energies of approximately 0.033 eV (270 cm^{-1}) for each multiplet line. The frequencies of the absorption maxima are given in the second column of Table II. Except for the intensity of the 3.84-eV absorption, the spectra of the solution and of the thin film are quite similar.

TABLE II. Observed electronic absorption maxima in (DMeFc)(TCNQ) (eV).

Acetonitrile solution by optical absorption	Monomeric phase		Dimeric phase conductivity	
	Optical absorption	Electron-energy loss	$\vec{E} \parallel \vec{a}$	$\vec{E} \parallel \vec{b}$
1.45[a]	1.35[a]	1.48[a]	1.23	1.21
1.66	1.62	1.68	1.88	1.85
2.95	2.95	2.40	2.6	
	3.16	3.15	3.27	3.27
3.84	3.74	3.85		
4.46	4.44	4.55		
		6.30		
		7.75		

[a]Only the energy of the main peak and its strongest vibronic sideband are given.

C. Electron-energy-loss spectra of the monomeric phase

Energy loss spectra of the strong $TCNQ^-$ monomer band are given in Fig. 5 as a function of momentum transfer q. Due to the resolution limit of 0.11 eV these spectra show only two peaks, corresponding to the main electronic excitation and its strongest vibrational sideband. However, the low-q energy-loss spectrum differs profoundly in shape from the optical-absorption spectrum in that the higher-energy vibrational sideband at 1.68 eV appears stronger than the main electronic transition at 1.48 eV. Moreover, as q increases to 0.7 Å^{-1} the relative intensity of the two components is reversed. A proper understanding of this change lies in the nature of the dielectric response of strong electronic excitations and a simple model for this previously unobserved effect is given in the discussion section.

The energy-loss spectrum of higher-energy electronic transitions is shown in Fig. 6. The energies of the peaks are tabulated in the third column of Table II. Owing to the dielectric effects discussed below we expect peaks in the energy-loss function $\mathrm{Im}(-1/\epsilon)$ (where $\epsilon=\epsilon_1+i\epsilon_2$ is the complex dielectric function) to occur near minima of ϵ_1 whereas optical-absorption peaks occur near maxima of ϵ_2. Since the dielectric response function ϵ_1 always exhibits a local minimum at greater energy than a strong intramolecular excitation, energy-loss peaks should occur slightly higher in energy than associated peaks in ϵ_2. Comparison of optical and energy-loss results shows this to be generally the case but the strong influence of the changing refractive index n causes the shapes of the optical and energy-loss spectra to differ considerably. Complete identification of the absorption bands at 6.30 and 7.75 eV must await a detailed molecular-orbital calculation.

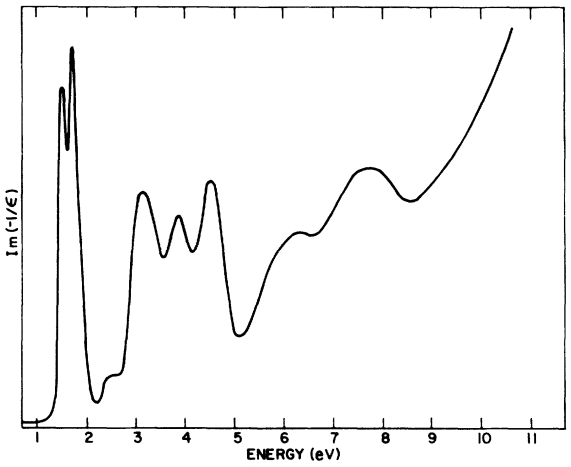

FIG. 6. Energy-loss spectra of the monomeric phase for $\vec{q}=0.15$ Å^{-1} from 0.6 to 11 eV.

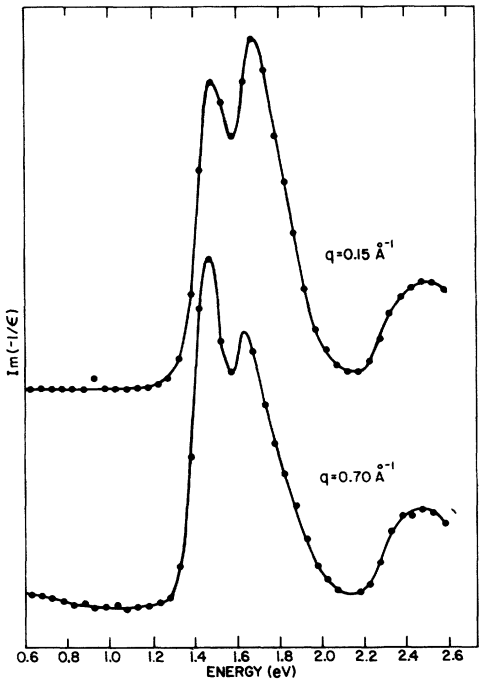

FIG. 5. Electron-energy-loss spectra for the monomeric phase between 0.6 and 2.7 eV. The data, for small and large values of the momentum transfer, are shown as points while the lines are intended as a guide to the eye.

D. Polarized reflectance

The growth habit of the dimeric (DMeFc)(TCNQ) crystals is such that the largest face contains the $\vec{a}$ and $\vec{b}$ crystallographic directions of the monoclinic unit cell[2] as shown in Fig. 1(b). There are two orthogonal sets of dimers in the crystal; in each set the dimer axis has components along all three of the crystallographic axes. The components along $\vec{a}$ and $\vec{b}$ are approximately (but not exactly) equal. Since these crystals have low symmetry, the dielectric function can be a tensor quantity, but because of the details of this complex structure, the anisotropy in the components is relatively small. One of the principal axes of the dielectric tensor will be along the b axis of the unit cell.

Figure 7 shows the reflectance of the dimeric complex with $\vec{E}\parallel\vec{a}$ and $\vec{E}\parallel\vec{b}$ from the infrared to the ultraviolet. Between 0.1 eV (800 cm^{-1}) and 0.3 eV (2400 cm^{-1}) are several sharp features associated with molecular vibrations. There are three broad maxima between 1 and 4 eV in both polarizations. The magnitude of the reflectance is relatively low, being between 0.02 and 0.08 over most of this region.

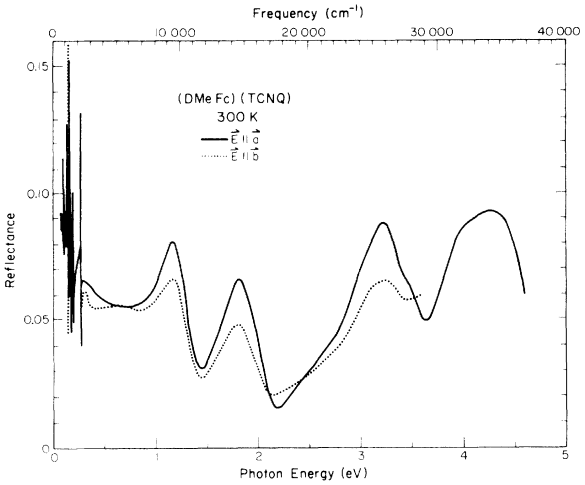

FIG. 7. Polarized reflectance of the dimeric phase of (DMeFc)(TCNQ) for $\vec{E} \parallel \vec{a}$ (solid line) and $\vec{E} \parallel \vec{b}$ (dotted line), between 0.1 and 4 eV.

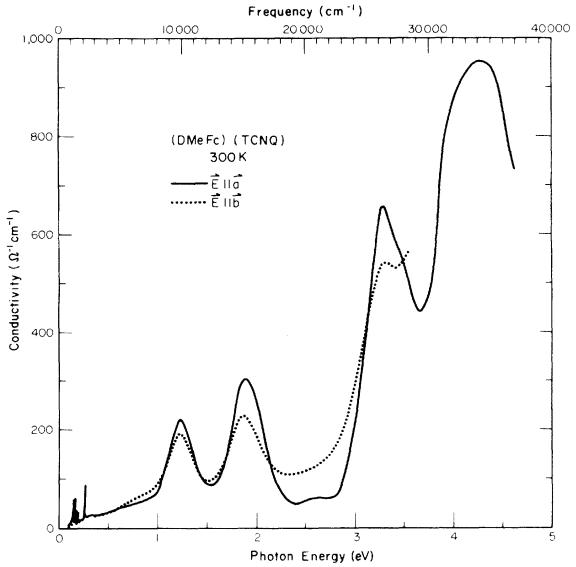

FIG. 8. Frequency-dependent conductivity, obtained by Kramers-Kronig analysis of the reflectance, for the dimeric phase of (DMeFc)(TCNQ). The conductivity for $\vec{E} \parallel \vec{a}$ is shown as a solid line while that for $\vec{E} \parallel \vec{b}$ is shown as a dotted line.

Because of the extremely wide frequency range covered, a Kramers-Kronig analysis of the reflectance should provide reasonably accurate values for the optical constants. In this procedure,[8] the phase shift upon reflectance $\theta(\omega)$ is given by an integral

$$\theta(\omega) = \frac{\omega}{\pi} \int_0^\infty \frac{\ln R(\omega') - \ln R(\omega)}{\omega^2 - \omega'^2} d\omega' \ , \qquad (1)$$

where R (ω) is the reflectance at frequency ω. Conventional extrapolation procedures were used in evaluating this integral. At low frequencies the reflectance was assumed to be constant. Between the highest data point and 25 eV the reflectance was extrapolated as $1/\omega^2$ to simulate interband transitions while above 25 eV a $1/\omega^4$ form appropriate for free-electron behavior was used.

Once the phase shift has been found from the Kramers-Kronig integral all of the optical functions can be calculated. Figure 8 shows the frequency-dependent conductivity $\sigma_1(\omega) = (\omega/4\pi)\epsilon_2$ over the whole frequency range studied. The energies of the maxima in $\sigma_1(\omega)$ give most closely the energies of electronic transitions in the solid. The frequencies of the conductivity maxima for both polarizations are given in the last two columns of Table II. The small differences for the two polarizations are probably not significant. The two lower transitions are of approximately equal strength, while the third one is 3–4 times their strength. The real part of the dielectric function $\epsilon_1(\omega)$ shows the usual derivativelike structure at frequencies near the conductivity maxima. Extrapolation of the infrared data to zero frequency gives a value of 3.3 ± 0.1 for the static dielectric constant.

Figure 9 shows the absorption coefficient and energy-loss function Im $(-1/\epsilon)$ for the dimeric crystals obtained from the Kramers-Kronig analysis. Only the data for $\vec{E} \parallel \vec{a}$ are depicted. These data should be compared to the film data of Figs. 4 and 6. The rather different optical properties of the two crystallographic forms are quite apparent and are consistent with the different structures.

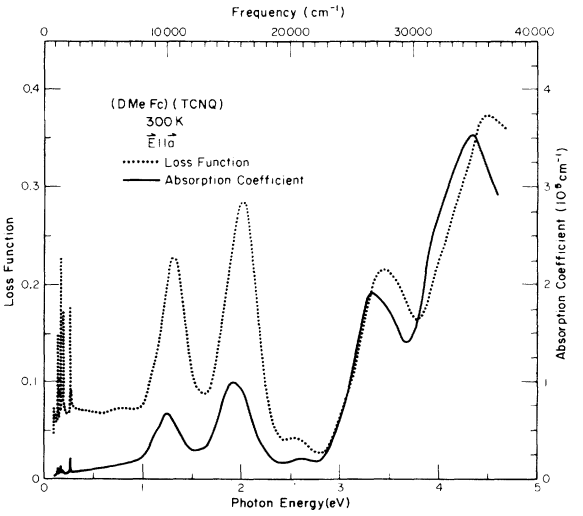

FIG. 9. Optical-absorption coefficient (solid line) and electron-energy-loss function (dotted line) for the dimeric phase of (DMeFc)(TCNQ), obtained by Kramers-Kronig analysis of the reflectance. The data are for $\vec{E} \parallel \vec{a}$ and are shown between 0.1 and 4.7 eV.

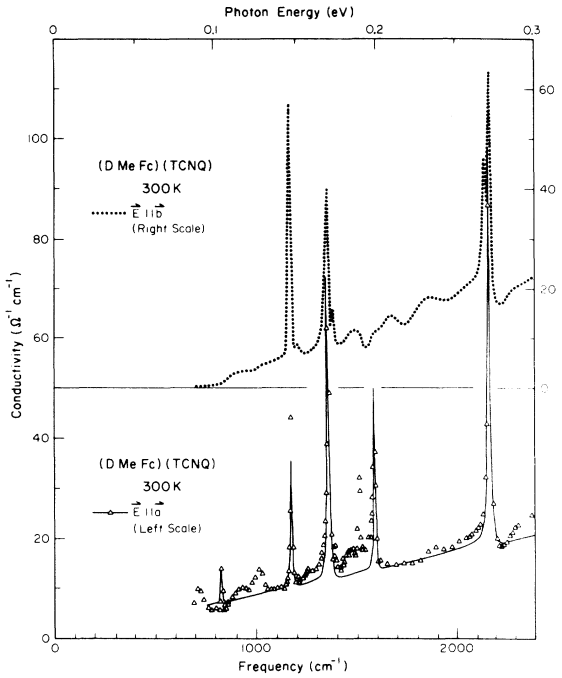

FIG. 10. Frequency-dependent conductivity of the dimeric phase of (DMeFc)(TCNQ) at low frequencies (between 0.1 and 0.3 eV). The data for $\vec{E}\|\vec{b}$ are shown as the upper dotted line while the actual data points for $\vec{E}\|\vec{b}$ are shown as triangles in the lower section of the figure. A fit of the theory of the electron-molecular vibration coupling in the dimer to the data for $\vec{E}\|\vec{b}$ is shown as the solid line.

The low-frequency part of the conductivity is shown in detail in Fig. 10. For $\vec{E}\|\vec{a}$ the data are shown as points. Comparing the two polarizations, there is some change of strength amongst the various modes [and some peaks for $\vec{E}\|\vec{b}$ may have been obscured in the water vapor band centered at 0.20 eV (1600 cm^{-1})] but the lines exhibit effects of electron-molecular vibrational coupling, as described below. The observed frequencies are given in the last two columns of Table I.

IV. DISCUSSION

A. Electronic transitions

The electronic structure of TCNQ has been the subject of numerous investigations, both theoretical and experimental.[4,5,7,9–22] The lowest-lying electronic transition of neutral TCNQ is observed[9] to occur at 2.8 eV. When the TCNQ radial anion is formed, as in the monomeric phase of $(DMeFc^+)(TCNQ^-)$, the extra electron goes into a previously vacant TCNQ molecular orbital of b_{2g} symmetry. This electron participates in the characteristic $TCNQ^-$ monomer absorption shown in Figs. 3 and 5. This absorption, first seen in solution by Boyd and Phillips,[4] is expected to be polarized along the TCNQ long axis and shows a characteristic vibronic splitting. The lowest-energy maximum in the absorption coefficient is at 1.35 eV while the center of the line is at 1.40 eV. These energies are somewhat lower than the energies of the same excitation in solution. The observation of this excitation in the (DMeFc)(TCNQ) monomeric phase is the first such observation in solid state. The monomer excitation is not observed in most TCNQ charge transfer salts because either the $TCNQ^-$ anions dimerize or donor-acceptor charge transfer excitations dominate the optical response. In the monomeric phase of (DMeFc)(TCNQ), on the other hand, truly isolated $(TCNQ)^-$ monomers are present and this excitation occurs in the spectrum.

When two $TCNQ^-$ radical ions are brought together to form a dimer, interactions between the ions may be observed. The theory of the dimer interaction has been described, in terms of the Hubbard model, by Harris and Lange[23] and recently by Rice.[24] This theory is concerned with the effects of the interaction within the dimer of the singly occupied π molecular orbitals of the two $TCNQ^-$ ions. The two parameters in the theory are the overlap matrix element or transfer integral t and the on-site Coulomb interaction U. The transfer integral describes the overlap of electronic wave functions between the adjacent molecules while the Coulomb interaction represents the net cost of having both electrons occupy the same molecular orbital.

In the presence of these interactions the original energy level of the monomer splits into four levels in the dimer. The ground state is a bonding arrangement with one electron on one molecule and the other electron, with opposite spin, on the other molecule. The next higher level, split by $\Delta_\chi = (U^2/4 + 4t^2)^{1/2} - \frac{1}{2}U$, is a triplet state having one electron on each molecule but with parallel spins. Above this triplet level is a state characterized by having two electrons (with opposite spin) localized on one of the two molecules. This "charge transfer" state is the only level coupled by the electric dipole operator to the ground state, and is at an energy

$$E_{CT} = \tfrac{1}{2}U + (U^{2/4} + 4t^2)^{1/2} \tag{2}$$

above the ground state. Finally, the highest level is the antibonding version of the ground state.

Within this theory there is an optical charge transfer excitation, polarized along the axis joining the two molecules, at a frequency $\omega_{CT} = E_{CT}/\hbar$. The dielectric tensor has been derived by Rice[24] and is given by

$$\vec{\epsilon}(\omega) = \vec{\epsilon}_\infty + \vec{A}\frac{4\pi n e^2 a^2}{\hbar^2}\frac{4t^2/(U^2/4 + 4t^2)^{1/2}}{\omega_{CT}^2[1 - D(\omega)] - \omega^2 - i\omega\gamma_e}, \tag{3}$$

where n is the density of molecules, a is the intradimer molecular separation, γ_e is a phenomenological linewidth, and $\vec{\bar{A}}$ gives the tensorial character to the dielectric function. If $\vec{a}_j$ is the vector joining the centers of the jth dimer, then $\vec{\bar{A}} = 1/N \sum_{j=1}^{N} \vec{a}_j \vec{a}_j / a_j^2$. Finally, as we shall see below, the function $D(\omega)$ in the denominator of Eq. (3) describes the effects arising from the coupling of the unpaired electron to the internal vibrations of the molecule. In the region of the electronic excitations, however, $D(\omega) \ll 1$ so that this function may be disregarded in the present discussion.

The frequency-dependent conductivity of this charge transfer excitation has an oscillator strength, found by integrating the conductivity over the charge transfer band, given by

$$\int_{CT} \vec{\sigma}_1(\omega)\, d\omega = \vec{\bar{A}} \frac{\pi n e^2 a^2}{\hbar^2} \frac{2t^2}{(U^2/4 + 4t^2)^{1/2}} \quad . \tag{4}$$

Provided that the quantities a, n, and $\vec{\bar{A}}$ are known, Eqs. (2) and (4) indicate that the parameters t and U can be found from optical data. For dimeric $(DMeFc^+)_2(TCNQ)_2^{2-}$, $a = 3.47$ Å, $n = 1.44 \times 10^{21}$ $TCNQ^-$anions/cm^3 and the diagonal components of $\vec{\bar{A}}$ along the a and b crystallographic axes are[25] $A_{aa} \simeq A_{bb} = 0.45$. Using these values and the data for $\sigma_1(\omega)$ in Fig. 7 we obtain $U = 1.0$ eV and $t = 0.27$ eV.

These values are not particularly surprising, being close to the commonly accepted values for the two quantities. The theory[24] described in the preceding paragraphs is an exact solution of the Hubbard model applied to the dimer and gives the energy and oscillator strength of the charge transfer excitation. In the dimeric phase of (DMeFc)(TCNQ), there occur well-isolated TCNQ dimers. We thus have a simple exact theory and a model system to which to apply it. In addition, the theory gives the energy between the singlet and the triplet excitation levels. This energy can be observed as the activation energy for magnetic susceptibility and we predict it to occur at $\Delta_\chi = 0.23$ eV, corresponding to an activation temperature of 2600 K.

The above discussion of the dimer electronic structure has been based on a consideration of only the singly occupied $TCNQ^-$ b_{2g} molecular orbital. The effects which give the absorption in the monomeric phase should be present in the dimer also, although interaction between the two excitation states would be expected to raise the energy of this local exciton. This exciton is seen in Fig. 7 at 1.9 eV. In the dimer this band is totally free of any vibronic coupling.

Similar effects have been previously observed in solution where dimer formation can take place.[4,16] In solution the dimer local exciton is at ~2.0 eV with no vibronic structure. Several linear chain TCNQ salts which have dimerized stacks show absorption peaks at this energy along with a charge transfer band at lower energy. A variety of dimer systems have been studied[14–16,18–21] and although solid-state effects such as a tendency to band formation are likely to be important, the strongly dimerized salts, such as Li (TCNQ), K(TCNQ), phase-I Rb (TCNQ), etc., all show absorption maxima at ~1.1, ~1.95, and ~3.3 eV corresponding approximately to the charge transfer mode and two localized excitons of the TCNQ molecules.

B. Momentum dependence

In organic molecular solids where electronic energy bandwidths are expected to be of the order of 0.1 eV no momentum dependence of the localized intramolecular excitations is expected. However, in solid TCNQ° and polystyrene a definite q-dependent change in the energy-loss peak position and spectral shape has been observed.[26,27] In TCNQ° where a large difference of the transverse and longitudinal exciton energies occurs the q-dependent spectral changes were thought to be due either to the negative dispersion of the longitudinal exciton or to q-dependent local-field effects.[26] In polystyrene where no large exciton splitting is observed, the energy-loss spectrum has been qualitatively accounted for with a local-field-effect model.[27] In the q-dependent spectra reported here for films of the monomeric phase, an unusual shape change with increasing q is simply described as a dielectric effect due to the decreasing strength of an intramolecular excitation with momentum transfer.

The optical-absorption coefficient is $\alpha = (2\omega/c)k$, where k is the imaginary part of the index of refraction $N = n + ik$. The energy-loss probability is proportional to $\mathrm{Im}(-1/\epsilon) = \epsilon_2/(\epsilon_1^2 + \epsilon_2^2)$ where $\epsilon = N^2$ is the dielectric response function with real and imaginary parts ϵ_1 and ϵ_2. If one measures k over a large enough energy region one can calculate the real part of the index of refraction n at energy E by the Kramers-Kronig relation

$$n(E) = 1 + \frac{2}{\pi} \mathrm{P} \int_0^\infty k(E') \frac{E'\, dE'}{E'^2 - E^2} \quad , \tag{5}$$

where P indicates the Cauchy principal value. Given n and k one can calculate the expected energy-loss function. The computation is simplified by noting that for a relatively isolated band such as seen in Figs. 3 and 6 cutting off the integral just above the band introduces no new structure into $n(E)$ in the region of the band and merely reduces all values of $n(E)$ by an additive constant. Including this constant is seen to change the amplitude but not the shape of the predicted energy-loss spectrum. From the thin-film absorption coefficient of Fig. 3 the refractive index was calculated using the Kramers-Kronig integral

[Eq. (5)]. From n and k, the expected energy-loss function $\mathrm{Im}(-1/\epsilon)$ was determined. The result is shown as the center curve of the left-hand side of Fig. 11, which is labeled by a parameter which indicates an arbitrary multiplicative factor for the measured k. Note that the strength of the strongest vibrational sideband is increased in the energy-loss function relative to that in the optical-absorption spectrum but that it does not truly represent the low-q energy-loss spectrum shape as it should. (The additional fine structure in the calculated energy-loss spectrum is smoothed out in the measured spectrum by the 0.11-eV resolution.) Since the absorption of $TCNQ^-$ monomers is polarized along the long axis the measured k in a polycrystalline film could be low by a factor of 3 compared with a single oriented crystal. Thus, we have arbitrarily multiplied k by a factor of 2 and 3, and computed the energy-loss functions as the upper curves on the left side of Fig. 11. The relative strength of the higher-energy component

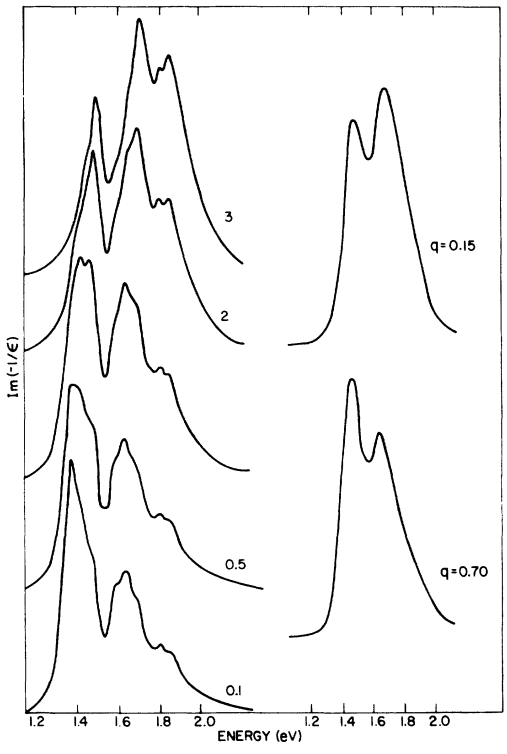

FIG. 11. Electron-energy-loss spectra computed from the measured optical-absorption coefficient of the monomeric phase of (DMeFc)(TCNQ) are shown on the left side of the figure. These spectra should be compared with the measured loss function at small and large values of the momentum transfer q shown on the right side of the figure. The number next to each calculated curve indicates the factor by which the extinction coefficient k was multiplied before calculating the refractive index n from the Kramers-Kronig relation.

more nearly agrees with the small-q energy-loss spectrum shape as indicated on the right-hand side of Fig. 11. Even though the energy-loss spectra were also obtained on polycrystalline films this correction to k is reasonable because the shape of the energy-loss spectra from a polycrystalline array will resemble the single oriented crystal spectrum since other crystalline directions do not contribute to the loss spectrum in this energy region. Thus, although the shape of the absorption spectrum does not change, profound changes in $\mathrm{Im}(-1/\epsilon)$ can occur if the amplitude or strength of an absorption band is varied since the refractive index n changes radically if k is large. Herein lies the key to a simple understanding of the q dependence of this absorption band. As q is increased, the strength of any single electric dipole transition must decrease, since at large q higher-energy dipole forbidden excitations always occur, and the total integrated oscillator strength in an energy-loss spectrum is constant.[26,27] This q-dependent decrease in oscillator strength can be simulated by arbitrarily reducing k and recomputing the energy-loss function. The result of multiplying k by 0.5 and 0.1 is shown in Fig. 11 as the bottom-left-hand energy-loss curves which compare well with the overall shape of the $q = 0.7\,\text{Å}^{-1}$ measured energy-loss spectrum. Thus, although local-field and excitonic effects are undoubtedly important, in this case a simple explanation for the momentum dependence of the energy-loss spectrum lies in the strength dependence of the dielectric response function.

C. Electron-molecular vibration coupling

Figure 10 shows that a series of narrow absorption bands are observed for the dimeric phase of (DMeFc)(TCNQ) in the region of molecular vibration frequencies. As discussed by Rice[24] such a series of bands is to be expected for the ion-radical dimer on account of electron-molecular vibration (EMV) coupling. In the monomer, the radical electrons couple to the totally symmetric (a_g) molecular vibrations of the monomer. In the dimer, the antisymmetric linear combinations of these vibrations couple directly to the charge transfer excitations, and, in consequence, drive oscillations in the radical electron electric dipole moment. These "dimer charge oscillations" give rise to an apparent infrared activity of the previous inactive (monomer) a_g modes, polarized in the direction of the dimer axis, an effect previously seen in K(TCNQ).[21,28] The effect is described by the function $D(\omega)$ present in Eq. (3), the function $D(\omega)$ being

$$D(\omega) = \sum_{\alpha=1}^{G} \frac{\lambda_\alpha \omega_\alpha^2}{\omega_\alpha^2 - \omega^2 - i\omega\gamma_\alpha} , \tag{6}$$

G is the number of modes in which ω_α denotes the

TABLE III. Electron-molecular vibration coupling parameters for dimeric (DMeFc)(TCNQ).

Mode α	Vibration frequency ω_α (cm^{-1})	Coupling constant g_α (meV)
2	2214	101
3	1610	67
4	1398	86
5	1186	43
6	829	20–30

frequency of the monomer a_g mode and γ_α its natural linewidth. The quantity λ_α is the dimensionless constant

$$\lambda_\alpha = \frac{16t^2}{(\hbar\omega_{CT})^2(U^2/4+4t^2)^{1/2}}\frac{g_\alpha^2}{\hbar\omega_\alpha} \quad (7)$$

and specifies the strength of electronic charge transfer molecular vibration coupling. In Eq. (7) g_α denotes the a_g monomer EMV coupling constant for the mode α. Typically, $\lambda_\alpha \sim 10^{-2}$.

We identify the six molecular absorption features appearing in $\sigma_1(\omega)$ for $\vec{E}\parallel\vec{a}$ (Fig. 10) as the dimer charge oscillations associated with the TCNQ monomer a_g modes.[29,30] At least-squares fit[31] of Eq. (3) to the data yields "experimental" values for the parameters ω_α, g_α, and γ_α and hence, in view of Eq. (7), for the a_g coupling constants g_α, since t and U are known from the analysis of Sec. IV A. The values of ω_α and g_α obtained from such a fit are given in Table III. In this fit, which is shown in Fig. 10, the natural linewidths γ_α of the a_g modes were all taken to be 6 cm^{-1}, while the steadily increasing background seen in the experimental data was simulated by using a complex value for the high-frequency dielectric function $\epsilon_\infty = 2.2 + 0.5i$. The values obtained for g_α are generally in agreement with those previously deduced[27] from polarized optical reflectance studies[21] of K(TCNQ) and with those theoretically calculated by Lipari and Duke.[30] However, the values $g_2 = 101$ meV we find for the electronic coupling to the $C \equiv N$ stretching mode $\omega_2 = 2214$ cm^{-1}, considerably exceed the theoretical value $g_2 = 52$ meV calculated by Lipari and Duke although it is more consistent with the experimental value $g_2 = 73$ meV deduced[27] for K(TCNQ). There are some differences between the spectra for $\vec{E}\parallel\vec{a}$ and $\vec{E}\parallel\vec{b}$ shown in Fig. 10. A fit to the smaller number of lines observed for $\vec{E}\parallel\vec{b}$ would yield somewhat different values for the coupling contants. Some of these differences are due to experimental errors in part because the signal level is somewhat lower for $\vec{E}\parallel\vec{b}$ than for $\vec{E}\parallel\vec{a}$. At the present time we can offer no definite explanation of these differences.

V. SUMMARY AND CONCLUSIONS

These measurements have shown that the existence of two dissimilar crystallographic phases make (DMeFc)(TCNQ) a novel system for the study of the solid-state properties of the TCNQ radical ion. In the monomeric phase the excitation spectrum of the isolated ion has been measured. The most notable feature is the extremely strong vibronic coupling of the lowest-energy transition at 1.4 eV. This transition has previously only been studied in solution.[4,5] In the dimeric phase a charge transfer band appears at 1.2 eV with the lowest intramolecular transition at 1.9 eV. Surprisingly, in the dimer this excitation is totally free of any structure due to vibronic interaction. The reason for the disappearance of the vibronic structure on going from the monomer to the dimer is not understood.

From an analysis of the charge transfer excitation in the dimeric phase we obtain values for the effective on-site Coulomb repulsion $U = 1.0$ eV, and for the transfer matrix element $t = 0.27$ eV. If these numbers are applied to linear-chain TCNQ systems, then the bandwidth would be $W = 4t \sim 1$ eV $\sim U$. These systems would be in the intermediate Coulomb correlation case.

ACKNOWLEDGMENTS

We thank A. H. Reis, Jr. for providing information and descriptions of the structure of both the monomeric and the dimeric phases. D. B. T. thanks Dr. F. J. Dickey for the loan of the grating monochromator.

*Current address: Occidental Research Corp., Irvine, California 92713.

[1]J. S. Miller, A. H. Reis, Jr., E. Gebert, J. J. Ritsko, W. R. Salaneck, L. Kovnat, T. W. Cape, and R. P. Van Duyne, J. Am. Chem. Soc. 101, 7111 (1979).

[2]A. H. Reis, Jr., L. D. Preston, J. M. Williams, S. W. Peterson, G. A. Candela, L. Swartzendruber, and J. S. Miller, J. Am. Chem. Soc. 101, 2756 (1979).

[3]G. Candela, L. J. Swartzendruber, J. S. Miller, and M. J. Rice, J. Am. Chem. Soc. 101, 2755 (1979).

[4]R. H. Boyd and W. D. Phillips, J. Chem. Phys. 43, 2927 (1965).

[5](a) I. Heller and F. B. Kaufman, J. Am. Chem. Soc. 98, 1464 (1976); (b) F. B. Kaufman and I. Heller, Chem.

Phys. Lett. 33, 30 (1975).
[6]D. M. Duggan and D. M. Hendrickson, Inorg. Chem. 14, 955 (1975).
[7]N. O. Lipari, Paul Nielsen, J. J. Ritsko, A. J. Epstein, and D. J. Sandman, Phys. Rev. B 16, 1000 (1977).
[8]Frederick Wooten, *Optical Properties of Solids* (Academic, New York, 1972), Appendix G.
[9]R. R. Pennelly and C. J. Eckhardt, Chem. Phys. 12, 89 (1976).
[10]D. A. Lowitz, J. Chem. Phys. 46, 4698 (1967).
[11]F. Herman, A. R. Williams, and K. H. Johnson, J. Chem. Phys. 6, 3508 (1974).
[12]H. T. Jonkman, G. A. Van der Welde, and W. C. Niewport, Chem. Phys. Lett. 25, 62 (1975).
[13]J. Hubbard, Phys. Rev. B 17, 494 (1978).
[14]Y. Iida, Bull. Chem. Soc. Jpn. 42, 71 (1969).
[15]S. Hiroma, H. Kuroda, and H. Akamatu, Bull. Chem. Soc. Jpn. 44, 9 (1971).
[16]Y. Oohashi and T. Sakata, Bull. Chem. Soc. Jpn. 46, 765, 3330 (1973); 48, 1725 (1975).
[17]A. Brau, P. Brüesch, J. P. Farges, W. Hinz, and D. Kuse, Phys. Status Solidi B 62, 615 (1974).
[18]J. G. Vegter and J. Kommandeur, Phys. Rev. B 9, 5150 (1974).
[19]J. B. Torrance, B. A. Scott, and F. B. Kaufman, Solid State Commun. 17, 1369 (1975).
[20]J. Tanaka, M. Tanaka, T. Kawai, T. Takaba, and S. Maki, Bull. Chem. Soc. Jpn. 49, 2358 (1976).
[21]D. B. Tanner, C. S. Jacobsen, A. A. Bright, and A. J. Heeger, Phys. Rev. B 16, 3283 (1977).
[22]K. Kamarás, G. Grüner, and G. A. Sawatzky, Solid State Commun. 27, 1171 (1978).
[23]A. Brooks Harris and Robert V. Lange, Phys. Rev. 157, 295 (1967).
[24]M. J. Rice, Solid State Commun. 31, 93 (1979).
[25]A. H. Reis, Jr. (private communication).
[26]J. J. Ritsko, N. O. Lipari, P. C. Gibbons, S. E. Schnatterly, J. R. Fields, and R. Devaty, Phys. Rev. Lett. 36, 210 (1976).
[27]J. J. Ritsko, J. Chem. Phys. 70, 4656 (1979).
[28]M. J. Rice, N. O. Lipari, and S. Strassler, Phys. Rev. Lett. 39, 1359 (1977).
[29]A. Girlando and C. Pecile, Spectrochim. Acta Part A 29, 1859 (1973).
[30]N. O. Lipari, M. J. Rice, C. B. Duke, R. Bozio, A. Girlando, and C. Pecile, Int. J. Quantum Chem. 11, 583 (1977).
[31]Philip R. Bevington, *Data Reduction and Error Analysis for the Physical Sciences* (McGraw-Hill, New York, 1969), Chap. 11.